



Factors governing the in vivo tissue uptake of transferrin-coupled polyethylene glycol liposomes in vivo

Hiroto Hatakeyama^{a,1}, Hidetaka Akita^{a,1}, Kazuo Maruyama^b,
Tetsuya Suhara^{c,1}, Hideyoshi Harashima^{a,*,1}

^a *Laboratory for Molecular Design of Pharmaceutics, Graduate School of Pharmaceutics,
Hokkaido University, Sapporo, Hokkaido 060-0812, Japan*

^b *Faculty of the Pharmaceutical Sciences, Teikyo University, Sagamiko, Tsukui-gun, Kanagawa 199-0195, Japan*

^c *National Institute of Radiological Sciences, 4-9-1, Anagawa, Inage-ku, Chiba-Shi, 263-8555, Japan*

Received 6 March 2004; received in revised form 24 April 2004; accepted 15 May 2004

Abstract

Liposomes, coated with transferrin (Tf)-coupled polyethylene glycol are considered to be potent carriers for drug delivery to various organs via receptor-mediated endocytosis. Since Tf receptors were ubiquitously expressed in various organs, additional perturbation of the liposomes such as regulation of the size may be required to exhibit the tissue selectivity. In the present study, the effect of size on the uptake of transferrin-coupled polyethylene glycol liposomes (Tf-PEG-L) to various organs was investigated. In liver and brain, Tf-dependent uptake was found to be dependent on the size of the liposomes used. In small liposomes with a diameter of 60–80 nm, Tf-PEG-L was taken up to these organs more efficiently than PEG-L. This Tf-dependent uptake for small liposomes decreased by the high dose administration, suggested that Tf-PEG-L is taken up via Tf receptor-mediated endocytosis even under the physiological condition, in which plasma concentration of endogenous Tf remains high. On the other hand, Tf receptor-mediated uptake was also observed in the heart, but size-dependency was not observed in this case. Collectively, these results indicate that size dependency in the uptake of Tf-PEG-L is tissue-dependent and therefore, controlling the size of Tf-PEG-L may be useful for the success of tissue targeting.

© 2004 Elsevier B.V. All rights reserved.

Keywords: Transferrin; Liposomes; Receptor-mediated endocytosis; Tissue uptake

1. Introduction

Liposomes coated with polyethyleneglycol (PEG-L) have shed light on their use as potent drug carriers, since these have the ability to escape from the reticuloendothelial system (RES) and to circulate in the blood for a long period (Blume and Cevc,

1990; Klibanov et al., 1990; Allen and Hansen, 1991; Klibanov et al., 1991; Mori et al., 1991; Litzinger et al., 1994; Maruyama et al., 1999). In addition, various ligands or antibodies can be further attached to the surface-granted PEG chains, thus permitting them to be actively taken up by the target cells via receptor-mediated endocytosis (Maruyama et al., 1999). One example is transferrin (Tf), whose receptors are ubiquitously expressed in various tissues including the luminal membrane of the brain capillary endothelium, and tumor cells have also been used for targeting (Ponka and Lok, 1999; Qian et al., 2002). Partridge

* Corresponding author. Tel.: +81-11-706-3919;
fax: +81-11-706-4879.

E-mail address: harasima@pharm.hokudai.ac.jp (H. Harashima).

¹ Advanced and Innovational Research Program in Life Sciences.

and co-workers developed immunoliposomes against this receptor, and succeeded in the delivery of anticancer drugs (e.g. doxorubicin), oligo DNA and plasmid DNA to the brain via receptor-mediated transcytosis (Liu et al., 1992; Huwyler et al., 1996, 1997; Pardridge, 1999; Lee et al., 2000, 2002a,b; Shi et al., 2000, 2001; Shi and Pardridge, 2000).

In addition, Ishida et al. (2001) demonstrated the utility of Tf-coupled PEG liposomes (Tf-PEG-L) for the intracellular targeting of the liposomes to tumor cells via receptor-mediated endocytosis. They also showed that small liposomes with a diameter of 60 nm were taken up by tumor cells by receptor-mediated endocytosis, but not those of 120 nm. Considering that the majority of the coated vesicles were less than 100 nm (Steven et al., 1983), sizing of ligand-coupling PEG liposomes that are below this threshold is also essential for successful intracellular targeting. To investigate whether this rule can be also applied to normal tissues, we kinetically evaluated the uptake of differently sized PEG-L and Tf-PEG-L. In the present study, we raise finding that size dependency in the uptake of Tf-PEG-L is tissue-dependent and therefore, regulation of the size of liposomes may lead to the tissue targeting.

2. Materials and methods

2.1. Materials

Cholesterol (CH) and distearoyl-*sn*-Glycero-3-phosphoethanolamine-*N*-[methoxy (polyethylene glycol)-2000] (DSPE-PEG) were purchased from Avanti Polar Lipids, Inc. (Alabaster, AL). DSPE-PEG with a functional maleimide moiety at the terminal end of PEG: *N*-[(3-maleimide-1-oxopropyl)aminopropyl polyethyleneglycol-carbamyl] distearoylphosphatidylethanolamine (DSPE-PEG-Mal) and egg phosphatidylcholine (EPC) were purchased from Nippon Oil and Fat Co. (Tokyo, Japan). [cholesteryl-1,2-³H(*N*)]-cholesteryl hexadecyl ether ([³H]CHE) and [³H]inulin was purchased from Perkin-Elmer Life Science Japan (Tokyo, Japan). Human holo-Tf and 3-(2-pyridyldithiopropionic acid *N*-hydroxy-succinimide ester (SPDP) were purchased from Sigma (St. Louis, MO). Male ddy mice (5–6 weeks old) were purchased from Sankyo Labo Service (Sapporo, Japan).

2.2. Preparation of PEG-L and Tf-PEG-L

PEG-L was prepared from EPC, CH, and DSPE-PEG in a molar ratio of 2:1:0.18. [³H]CHE and [³H]inulin were used as a lipid phase marker and an aqueous phase marker, respectively. Different sizes of liposomes were prepared by a reverse phase evaporation method, followed by extrusion with an Avanti Mini-Extruder. To prepare large liposomes with a size of 140–180 nm, liposomes were extruded through polycarbonate membrane filters (pore size of 0.2 μ m) 19 times. To prepare small liposomes with a size of 60–80 nm, large liposomes were further extruded through polycarbonate membrane filters having pore size of 0.1 and 0.05 μ m for 19 times each. The distribution of liposome diameter was determined by a dynamic laser scattering method with an ELS-8000HO instrument (Otsuka Electronics, Osaka, Japan).

Concerning the Tf-PEG-L, EPC, CH, DSPE-PEG and DSPE-PEG-Mal were first mixed at molar ratios of 2:1:0.15:0.03, and liposomes were prepared, as described above. Prior to this, Tf was modified with SPDP. A 20 mM solution of SPDP in methanol was reacted with the Tf (approximately 60 nmol), dissolved in PBS (pH 7.4) by stirred for 30 min at room temperature. The product was purified by chromatography on Sephadex G25. Dithiothreitol (DTT) was then added to the Tf-SPDP, at a final concentration of 50 mM, followed by 30 min incubation in the dark, to reduce the SPDP to permit it to react with the maleimide moiety on the surface of the PEG-liposome. After the separation of the product using Sephadex G25, the reduced Tf was incubated with the liposomes over night at 4 °C. Tf-PEG-L was separated from the free Tf by Bio-Gel A1.5m (BioRad: Hercules, CA). Recovery of the liposomes and Tf was evaluated by a cholesterol *E*-test WAKO (Wako: Osaka, Japan) and a BCA protein assay kit (Pierce: Rockford, IL), respectively. Small and large liposomes would be expected to contain approximately 210 and 450 molecules per liposome, respectively.

2.3. Pharmacokinetic analysis of the Tf-PEG-L and PEG-L

The liposomes were injected into a ddy mouse via the tail vein. The doses of liposomes were fixed at 2 nmol lipid/g BW (low dose) or 36 nmol lipid/g BW

(high dose). At the indicated times, the mice were sacrificed and blood, brain, liver, spleen, skeletal muscle and lung were collected. After weighing the samples, blood and organ samples were solubilized in Soluene-350 (Perkin-Elmer Life Sciences) for 5 h at 50 °C. Blood samples were decolorized by H₂O₂. The radioactivities were determined by liquid scintillation counting, after adding 10 ml of scintillation fluid (Hionic Flour; Perkin-Elmer Life Sciences).

Data analysis was performed, as described in the previous study (Harashima et al., 1992a,b). Plasma concentrations at the indicated times, $C(t)$ are expressed as %ID (injected dose) per ml of blood radioactivity (%ID/ml). Pharmacokinetic parameters were determined by fitting the $C(t)$ to a mono-exponential equation, as follows, using a non-linear regression analysis by the MULTI program:

$$C(t) = A e^{-kt}$$

The areas under the blood concentration–time curve (AUC) were calculated based on the following equation:

$$\text{AUC} = \int_{0\text{h}}^{48\text{h}} C(t) dt = \frac{A}{k} (1 - e^{-k \times 48})$$

To clarify the distribution of liposomes in the body, the radioactivities in the various organ samples, X_{organ} were first measured (Fig. 1). However, these values included a contribution by liposomes in the vascular space as well as the tissue parenchyma (including the macrophages and the capillary endothelial cells) (X_{tissue}). Therefore, a correction was made for liposomes in the vascular space as follows:

$$X_{\text{tissue}} = X_{\text{organ}} - V_0 C(t)$$

where V_0 denotes the total volume of the vascular space and interstitial fluid, as determined by the radioactivities in the whole organ samples divided by the blood concentration 10 min after the i.v. injection of the [³H]CHE-labeled PEG-L. Except for the liver or spleen, the capillary in other organs consisted of the continuous capillary, in which the distances of the open junction was less than 4 nm. Therefore, V_0 represents the capillary volume since paracellular capillary permeability of PEG-L is negligible. The uptake clearance (CL) in various tissues at 48 h were calculated as follows:

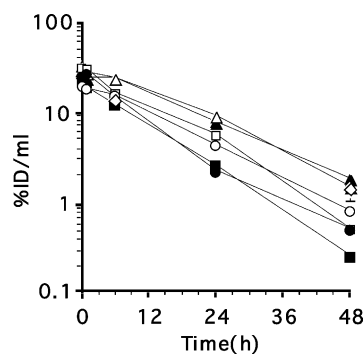


Fig. 1. Time profiles of the blood concentration of PEG-L and Tf-PEG-L. Open circles, closed circles, open squares and closed squares indicate the time profiles of the blood concentration, represented by %ID/ml of small PEG-L, small Tf-PEG-L, large PEG-L and large Tf-PEG-L, labeled with [³H]CHE after the administration of a low dose (2 nmol lipid/g BW), respectively. Open and closed triangles indicate the results of small PEG-L and Tf-PEG-L after the administration of a high dose (36 nmol/g BW), respectively. Blood concentration of small PEG-L labeled liposomes with the aqueous phase marker of [³H]inulin at 6 and 48 h are plotted as diamonds. Data are represented by the mean \pm S.E. ($n = 3$).

$$\text{CL} = \frac{X_{\text{tissue}}}{\text{AUC}}$$

This calculation is based on the assumption that the liposomes taken up by the organs were not effluxed to the blood in the present report (Lee et al., 2000), and it was supported by the experimental data (Harashima et al., 1992a).

3. Results and discussion

3.1. Plasma concentration and organ distribution of the PEG-L and Tf-PEG-L

For the optimization of the ligand-directed active targeting of the liposomes, the rapid elimination due to the nonspecific uptake by the reticuloendothelial system (RES) must be avoided. To overcome this barrier, PEG chains were attached to the surface of the liposomes (Blume and Cevc, 1990; Klibanov et al., 1990, 1991; Allen and Hansen, 1991; Mori et al., 1991; Litzinger et al., 1994; Maruyama et al., 1999), and ligands were coupled to the ends of the PEG chains. It has previously been determined that the Tf-dependent uptake of liposomes to tumor tissues only occurs for

Table 1
Kinetic parameters for the blood elimination of PEG-L and Tf-PEG-L

	C_0 (%ID/ml)	k (h^{-1})	$T_{1/2}$ (h)	Total body clearance (ml/h)
PEG-L (small, low)	19.9	0.067	10.3	9.72
Tf-PEG-L (small, low)	26.4	0.10	6.93	14.4
PEG-L (large, low)	28.4	0.078	8.90	11.2
Tf-PEG-L (large, low)	21.4	0.093	7.45	13.4
PEG-L (small, high)	31.9	0.063	10.9	9.16
Tf-PEG-L (small, high)	27.7	0.057	12.1	8.25

the small size (<60 nm), but not >120 nm liposomes (Ishida et al., 2001). This result prompted us to investigate the effect of size on the uptake of ligand-coupled PEG-L to normal tissues. In the present study, we have compared the disposition of PEG-L and Tf-PEG-L with small (the average diameter of 60–80 nm) and large (the average diameter of 140–180 nm) size.

First, time-profiles for the blood elimination of PEG-L and Tf-PEG-L labeled with [3 H]CHE were compared over a 48 h period (Fig. 1). As demonstrated previously (Ishida et al., 2001), Tf-PEG-L and PEG-L have a long circulation with a half-life of >6 h, and the total clearances of these liposomes are comparable regardless of size (Table 1). This suggests that modulation with Tf did not affect the RES uptake process. Furthermore, blood concentrations of PEG-L labeled with [3 H]CHE were compared to an encapsulating membrane-impermeable aqueous phase marker, [3 H]inulin in order to verify that the liposomes are intact even 48 h after i.v. administration. If [3 H]inulin were released from disintegrated liposomes, it would be rapidly eliminated from the body with a half-life of <5 min (data not shown). Therefore, [3 H]inulin that was not associated with liposomes had no effect on the blood concentration of the [3 H]inulin-labeled PEG-L. Since the encapsulation ratio of [3 H]inulin to the liposomes was limited, we injected [3 H]inulin-labeled PEG-L at a high dose (36 nmol lipid/g BW) to permit the detection of radioactivity, even at 48 h. As shown in Fig. 1, the blood concentrations of the [3 H]inulin-labeled liposomes at 6 and 48 h were comparable to the [3 H]CHE-labeled sample injected at a high dose, suggesting that the liposomes remained intact even at 48 h.

Organ distributions (X_{organ}) of PEG-L and Tf-PEG-L in the liver, spleen, lung, heart, skeletal muscle and brain were then evaluated 48 h after i.v. administration (Fig. 2). As shown previously, a large portion of the liposomes were recovered from the liver and spleen (>5% ID/g organ), suggesting that these are major clearance organs even for long circulating liposomes (Liu et al., 1992; Litzinger et al., 1994; Maruyama et al., 1999). As shown in the case of the tumor tissues, paracellular permeability partially contributes to the passive accumulation. In addition, active uptake mechanisms such as phagocytosis by Kupper cells in the liver, or filtration by a mesh-work consisting of reticular fibers and accompanying macrophages in the red pulp in spleen can be attributed to these high clearances, as reported previously (Klibanov et al., 1991; Litzinger et al., 1994). The uptake of the large PEG-L in spleen was further enhanced compared with small liposomes, presumably because large liposomes were efficiently trapped by filtration, as shown previously (Klibanov et al., 1991; Liu et al., 1992; Litzinger et al., 1994). Following these organs, lung, heart and muscle showed relatively high X_{organ} values (>0.5% ID/g tissue), while the brain was much lower (<0.1% ID/g tissue). It is generally thought that the blood brain barrier, constituting of the tight junction between the adjacent endothelial cells severely interrupts the movement of small molecules (Gloor et al., 2001; Huber et al., 2001; Wolburg and Lippoldt, 2002). Therefore, the extent of organ distribution of liposomes is presumably dependent on their permeability through the gap of the endothelial cells.

The uptake of liposomes from the blood to the tissues was then calculated based on the data shown in Figs. 1 and 2, and represented by the CL, in which the vascular space was corrected as described in Material and Method. In these calculations, the V_0 values in liver, spleen, lung, heart, muscle and brain were determined to be $219 \pm 28.5 \mu\text{l/g}$ liver, $141 \pm 34 \mu\text{l/g}$ spleen, $229 \pm 12 \mu\text{l/g}$ lung, $281 \pm 30 \mu\text{l/g}$ heart, $19.8 \pm 1.9 \mu\text{l/g}$ muscle and $20.2 \pm 0.5 \mu\text{l/g}$ brain, respectively by i.v. injection of [3 H]CHE-labeled PEG-L. The effects of size and dose on the tissue uptake of liposomes are shown in Figs. 3 and 4. Statistical differences, determined by one-way or two-way ANOVA followed by the Student–Newman–Keuls test are also summarized in Table 2.

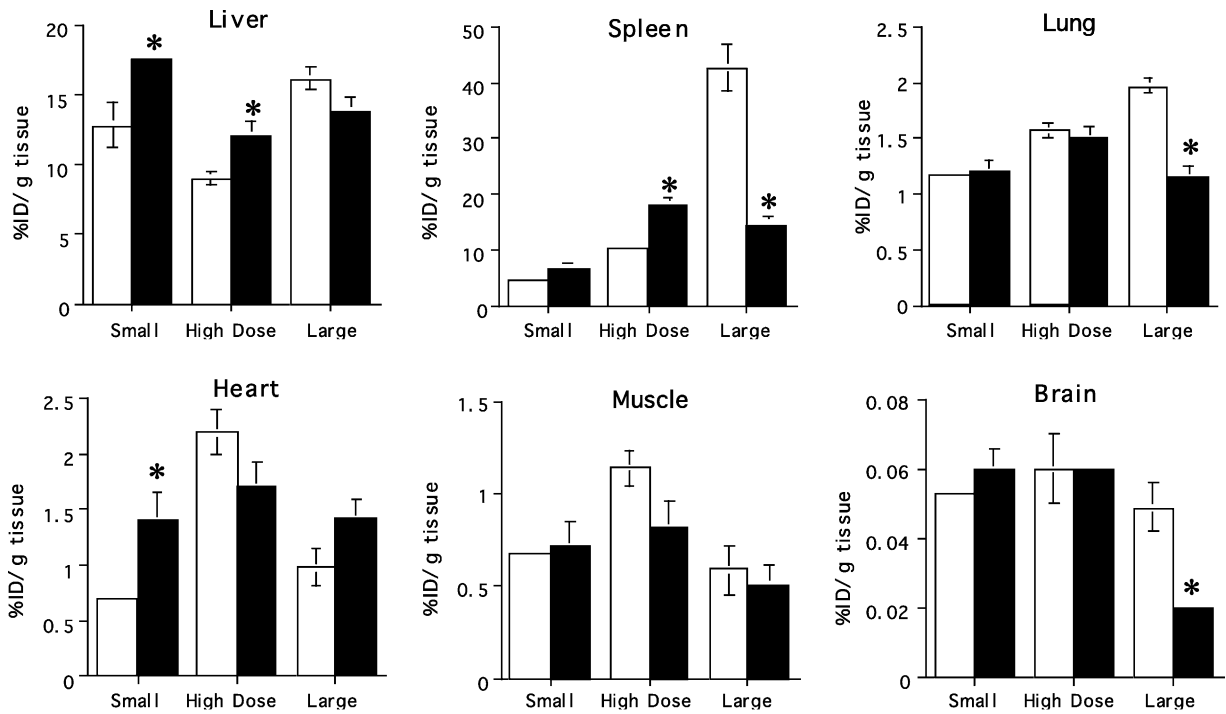


Fig. 2. The organ distribution of PEG-L and Tf-PEG-L. The organ distribution was expressed as the percentage injection dose per gram of organ (%ID/g organ), in liver, spleen, lung, heart, skeletal muscle and brain at 48 h after an i.v. injection of [³H]CHE labeled PEG-L and Tf-PEG-L. Open and closed bars indicate the results for PEG-L and Tf-PEG-L, respectively. Data are represented by the mean ± S.E. (n = 3). * Significantly different between PEG-L and Tf-PEG-L (P < 0.05 by Student's t-test).

Table 2
Summary of statistical analyses for of size- and dose-dependent uptake of the PEG-L and Tf-PEG-L

CL (μL/h/g tissue)	Tissue	Dose ^a	Size ^b	Tf-dependent tissue ^b uptake	
				Small	Large
>20	Liver	○	×	○ ^c	×
	Spleen	○	○	×	×
0.5–6	Lung	○	×	×	×
	Heart	×	×	○	○
	Muscle	×	×	×	×
0.05–0.2	Brain	○	○	○ ^c	×

^a The statistical differences of the size- and dose-dependent uptake of liposomes were determined by two-way ANOVA ((○) P < 0.05).

^b The statistical differences for the transferring-dependent uptake was determined by two-way ANOVA followed by Student–Newman–Keuls test ((○) P < 0.05).

^c The statistical differences for the transferring-dependent uptake was determined by one-way ANOVA followed by Student–Newman–Keuls test ((○) P < 0.05).

3.2. Effect of dose on the tissue uptake of the PEG-L and Tf-PEG-L

First, absolute values for the CL of small PEG-L injected at a low dose were compared among the various organs. Similar to the rank order of X_{organ} , values for CL were high in the liver and spleen (>15 μL/h/g tissue). As discussed above, active uptake such as entrapment by the Kupper cells in the liver and filtration by the meshwork of reticular fibers in the spleen may explain the high CL values found for the liver and spleen. With respect to the other organs, the CL value in the brain (<0.2 μL/h/g tissue) was much lower than that in the lung and muscle (1–4 μL/h/g tissue). Considering that the CL values were significantly reduced in various organs such as liver, lung and brain (Fig. 3 and Table 2), active uptake such as phagocytosis by the macrophages, or pinocytosis by the endothelial cells and/or tissue parenchyma may be involved.

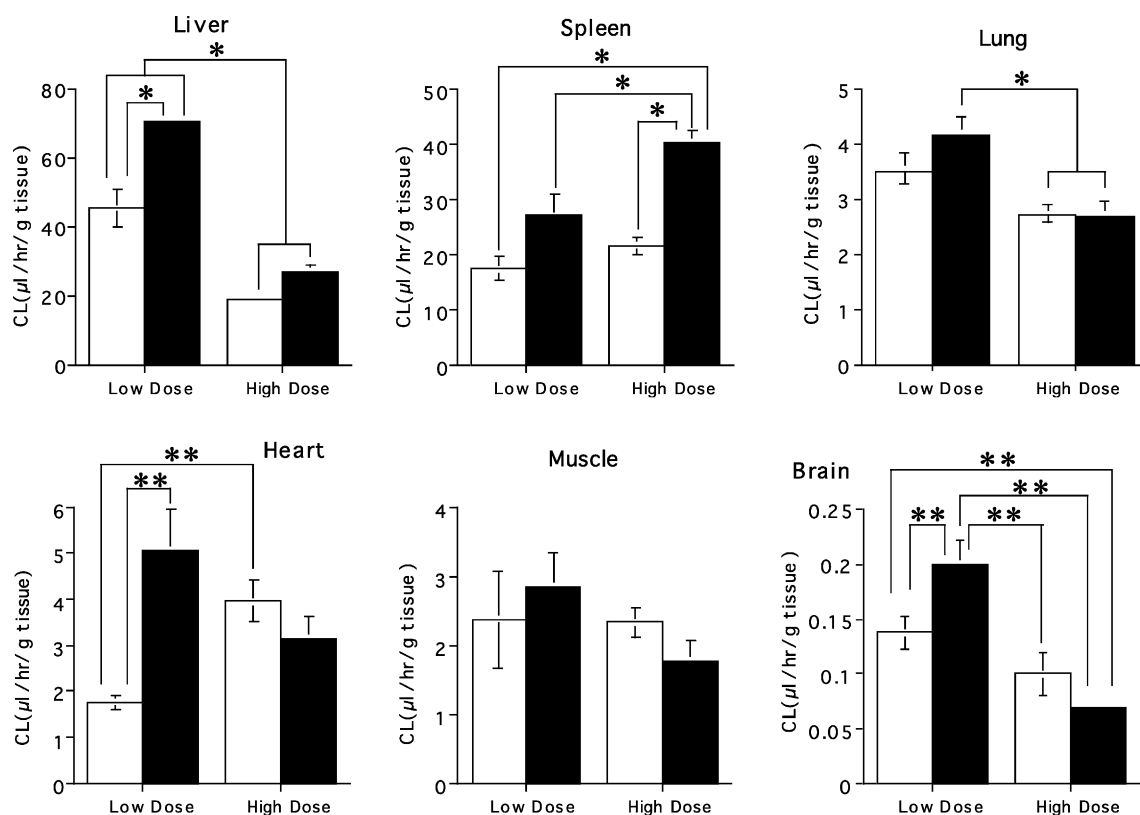


Fig. 3. Effect of liposomes dose on the uptake clearances. A comparison of the tissue uptake clearance by the various organs between a low dose injection (2 nmol lipid/g BW) and a high dose injection (36 nmol lipid/g BW). The uptake clearances for the small PEG-L (open bars) and Tf-PEG-L (closed bars) were calculated using the data in Figs. 1 and 2, as described in Section 2. Open and closed bars indicated results for PEG-L and Tf-PEG-L, respectively. Data are represented by mean \pm S.E. ($n = 3$). * Significantly different between PEG-L and Tf-PEG-L ($P < 0.05$ by two-way ANOVA, followed by Student–Newman–Keuls test). ** Significantly different between PEG-L and Tf-PEG-L ($P < 0.05$ by one-way ANOVA, followed by Student–Newman–Keuls test).

Then, the effect of the modulation of Tf was investigated. Considering that endogenous plasma concentration of Tf (approximately $10 \mu\text{M}$) is significantly higher than K_d values of Tf receptor (approximately 1 nM), they should be saturated under the physiological condition (Klausner et al., 1983). However, in the present study, Tf-dependent uptake was observed in the liver, brain and heart at low dose injection (2 nmol lipids/g body weight), and moreover, this effect is diminished by the administration of high doses of liposomes (36 nmol lipids/g body weight), suggesting that Tf-PEG-L was taken up by Tf receptor-mediated endocytosis (Fig. 3 and Table 2). In these conditions, initial (<6 h) concentration of the liposomes injected by low dose and high dose were estimated as 12.2 and 245 μM , respectively. These

values are converted to approximately 10 and 300 nM in terms of the Tf concentration modified on the Tf-PEG-L. These data can be accounted for by assuming that inhibition constant (K_i) of Tf against the Tf-PEG-L was significantly higher than K_d value of Tf receptors, since Tf-PEG-L exhibits the multivalent binding to the Tf receptors and high concentration of Tf are necessary to remove all of these binding. The values for the Tf-dependent uptake by these organs in liver ($\sim 25 \mu\text{l/h/g tissue}$), muscle ($\sim 4 \mu\text{l/h/g tissue}$) and brain ($\sim 0.05 \mu\text{l/h/g tissue}$) were quite different. This can be attributed to the differences in the density of Tf-receptors or internalization rate via endocytosis among these organs. In contrast, the uptake of Tf-PEG-L by the spleen was drastically enhanced when a high dose was injected, presumably because

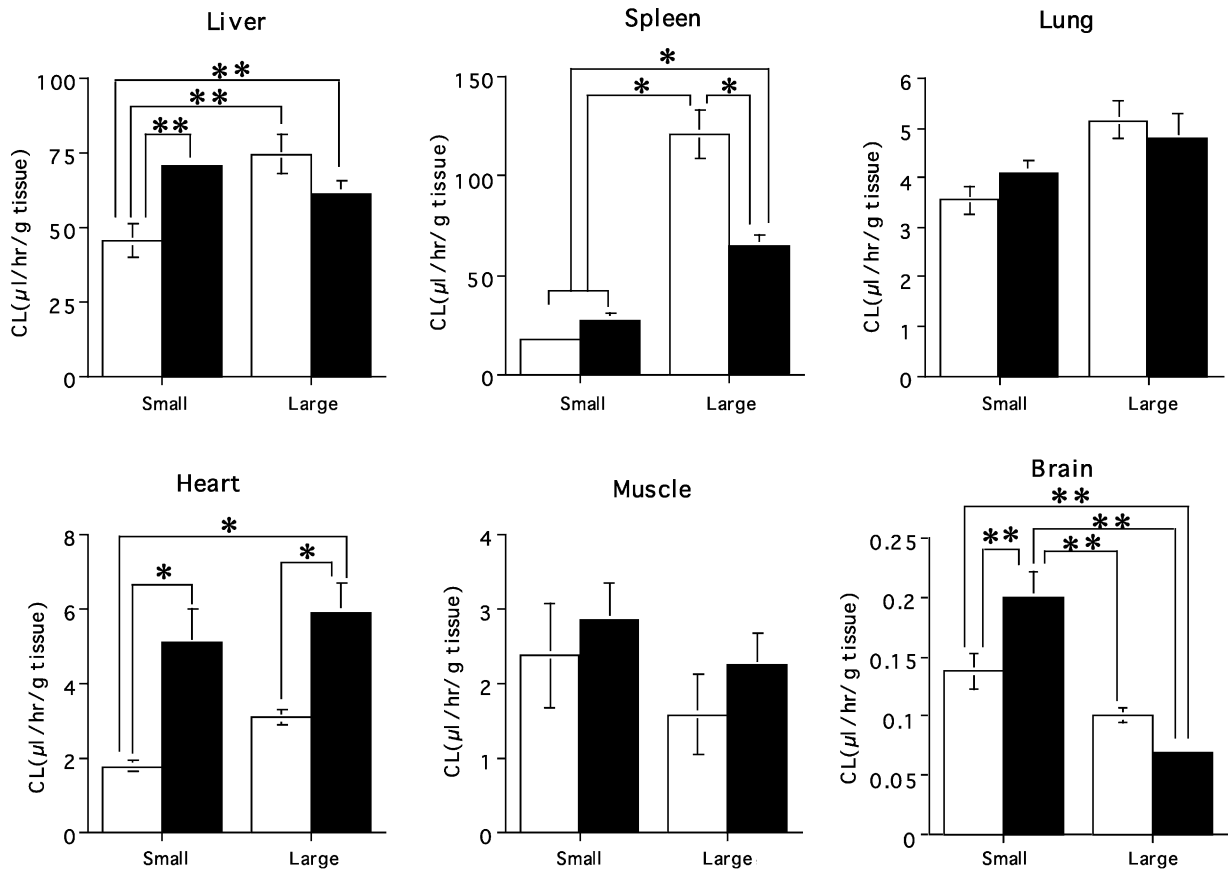


Fig. 4. Effect of liposome size on the uptake clearances. The uptake clearances of the small and large PEG-L (open bars) and Tf-PEG-L (closed bar) injected at a low dose (2 nmol lipid/g BW) were calculated using the data in Figs. 1 and 2 as described in Section 2. Open and closed bars indicate the results for PEG-L and Tf-PEG-L, respectively. Data are represented as the mean \pm S.E. ($n = 3$). * Significantly different between PEG-L and Tf-PEG-L ($P < 0.05$ by two-way ANOVA, followed by Student–Newman–Keuls test). ** Significantly different between PEG-L and Tf-PEG-L ($P < 0.05$ by one-way ANOVA, followed by Student–Newman–Keuls test).

of the immunogenesis derived from the human transferring attached to the PEG (Fig. 3 and Table 2).

On the other hand, in other organs such as lung and skeletal muscle, Tf-dependent uptake was barely detectable, in spite of the high or ubiquitous expression of Tf receptors (Ponka and Lok, 1999; Qian et al., 2002). These results are not in agreement with prior observations. It has been demonstrated that coupling of the antibody against Tf to a receptor (OX26) PEG liposomes are able to enhance accumulation by the spleen and lung in rats (Huwyler et al., 1997). Furthermore, PEG-L coupled with the OX26 monoclonal antibody is taken up by in vitro L6 cell cultures derived from skeletal muscle (Schnyder et al., 2003). In addition,

when antibodies against the Tf receptor were injected into the cynomolgous monkeys, a large portion of the dose was recovered from the skeletal muscle (Friden et al., 1996). These contradictions suggest that Tf is a much less potent ligand than OX26. In fact, the absolute value for the uptake of CL by the brain was approximately 1/15 of that of OX26 coupled PEG-L in rats (Huwyler et al., 1997)

3.3. Effect of size on the tissue uptake of the PEG-L and Tf-PEG-L

Finally, the effect of size on the tissue uptake of liposomes was investigated (Fig. 4 and Table 2). In

the heart and especially the spleen, the CL values for large liposomes were significantly increased over that of small liposomes. In addition, such a size-dependent uptake was also observed in the liver (e.g. small PEG-L versus large PEG-L), although the differences were not significant by two-way ANOVA. These findings are consistent with previous observations showing that larger liposomes are more susceptible to recognition by the complement system, followed by the phagocytosis by macrophages (Harashima et al., 1996). Therefore, entrapment by macrophages partially contributes to tissue uptake in these organs. In contrast, small liposomes were more extensively taken up by the brain. Presumably, pinocytosis, rather than phagocytosis plays a role in tissue uptake in the brain.

Concerning the hepatic uptake, Tf-dependent uptake was observed only for small liposomes, whereas no or little change was detected for large ones, suggesting that uptake via receptor-mediated endocytosis functions in the uptake of small liposomes with sizes less than 60–80 nm but not for the large ones because the major part of the diameter of the coated vesicles was less than 100 nm (Steven et al., 1983). This hypothesis is also supported by the fact that adenoviruses, with a diameter of 70–90 nm are able to efficiently access the liver parenchymal cells, resulting in a high level of transgene expression (Herz and Gerard, 1993). Such a size-dependent efficiency for endocytosis in vivo is also in agreement with an in vitro study showing that the internalization of large-sized cell-associated microspheres (200 nm) is substantially slower than that of small ones (50–100 nm) (Rejman et al., 2003). A size-dependent delay in uptake was also observed in viral particles (Matlin et al., 1982) and polyplexes (Godbey et al., 1999). Similarly, the Tf-dependent uptake of the liposomes was also observed only for the small liposomes by the brain, where Tf receptors are highly expressed on the luminal membrane of the endothelial cells. The uptake of Tf-PEG-L by brain capillary endothelial cells is consistent with previously reported microscopic observations (Omori et al., 2003). The size-dependent efficiency of clathrin-mediated endocytosis, as described above, also explains this result. In contrast to the liver and brain, Tf-dependent uptake by the heart was clearly observed and was independent of the size of the liposomes (Fig. 4). Although the mechanism remains to

be elucidated, smooth muscle cells in the heart may accept large particles via clathrin-coated vesicles.

4. Conclusion

In conclusion, a small size, less than 80 nm is an important factor for the tissue targeting of Tf-PEG-L based on receptor-mediated endocytosis, especially in the liver and brain. On the other hand, the heart is able to take up both small and large liposomes in a Tf-dependent manner. These results suggest that Tf can be the ligand for the active targeting of PEG-L in vivo even in the physiological condition, and regulation of size confer the tissue selectivity of Tf-PEG-L.

Acknowledgement

This study was performed through the Advanced and Innovational Research Program in Life Sciences from the Ministry of Education, Culture, Sports, Science and Technology, the Japanese Government.

References

- Allen, T.M., Hansen, C., 1991. Pharmacokinetics of stealth versus conventional liposomes: effect of dose. *Biochim. Biophys. Acta* 1068, 133–141.
- Blume, G., Cevc, G., 1990. Liposomes for the sustained drug release in vivo. *Biochim. Biophys. Acta* 1029, 91–97.
- Frیدن, P.M., Olson, T.S., Obar, R., Walus, L.R., Putney, S.D., 1996. Characterization, receptor mapping and blood-brain barrier transcytosis of antibodies to the human transferrin receptor. *J. Pharmacol. Exp. Ther.* 278, 1491–1498.
- Gloor, S.M., Wachtel, M., Bolliger, M.F., Ishihara, H., Landmann, R., Frei, K., 2001. Molecular and cellular permeability control at the blood-brain barrier. *Brain Res. Rev.* 36, 258–264.
- Godbey, W.T., Wu, K.K., Mikos, A.G., 1999. Tracking the intracellular path of poly(ethylenimine)/DNA complexes for gene delivery. *Proc. Natl. Acad. Sci. U.S.A.* 96, 5177–5181.
- Harashima, H., Komatsu, S., Kojima, S., Yanagi, C., Morioka, Y., Naito, M., Kiwada, H., 1996. Species difference in the disposition of liposomes among mice, rats, and rabbits: allometric relationship and species dependent hepatic uptake mechanism. *Pharm. Res.* 13, 1049–1054.
- Harashima, H., Kume, Y., Yamane, C., Kiwada, H., 1992a. Non-Michaelis-Menten type hepatic uptake of liposomes in the rat. *J. Pharm. Pharmacol.* 44, 707–712.
- Harashima, H., Ohshima, S., Midori, Y., Yachi, K., Kikuchi, H., Kiwada, H., 1992b. Kinetic analysis of tissue distribution of

- doxorubicin incorporated in liposomes in rats: I. Biopharm. Drug Dispos. 13, 155–170.
- Herz, J., Gerard, R.D., 1993. Adenovirus-mediated transfer of low density lipoprotein receptor gene acutely accelerates cholesterol clearance in normal mice. Proc. Natl. Acad. Sci. U.S.A. 90, 2812–2816.
- Huber, J.D., Egleton, R.D., Davis, T.P., 2001. Molecular physiology and pathophysiology of tight junctions in the blood-brain barrier. Trends Neurosci. 24, 719–725.
- Huwyler, J., Wu, D., Pardridge, W.M., 1996. Brain drug delivery of small molecules using immunoliposomes. Proc. Natl. Acad. Sci. U.S.A. 93, 14164–14169.
- Huwyler, J., Yang, J., Pardridge, W.M., 1997. Receptor mediated delivery of daunomycin using immunoliposomes: pharmacokinetics and tissue distribution in the rat. J. Pharmacol. Exp. Ther. 282, 1541–1546.
- Ishida, O., Maruyama, K., Tanahashi, H., Iwatsuru, M., Sasaki, K., Eriguchi, M., Yanagie, H., 2001. Liposomes bearing polyethyleneglycol-coupled transferrin with intracellular targeting property to the solid tumors in vivo. Pharm. Res. 18, 1042–1048.
- Klausner, R.D., Van Renswoude, J., Ashwell, G., Kempf, C., Schechter, A.N., Dean, A., Bridges, K.R., 1983. Receptor-mediated endocytosis of transferrin in K562 cells. J. Biol. Chem. 258, 4715–4724.
- Klibanov, A.L., Maruyama, K., Beckerleg, A.M., Torchilin, V.P., Huang, L., 1991. Activity of amphipathic poly(ethylene glycol) 5000 to prolong the circulation time of liposomes depends on the liposome size and is unfavorable for immunoliposome binding to target. Biochim. Biophys. Acta 1062, 142–148.
- Klibanov, A.L., Maruyama, K., Torchilin, V.P., Huang, L., 1990. Amphipathic polyethyleneglycols effectively prolong the circulation time of liposomes. FEBS Lett. 268, 235–237.
- Lee, H.J., Boado, R.J., Braasch, D.A., Corey, D.R., Pardridge, W.M., 2002a. Imaging gene expression in the brain in vivo in a transgenic mouse model of Huntington's disease with an antisense radiopharmaceutical and drug-targeting technology. J. Nucl. Med. 43, 948–956.
- Lee, H.J., Engelhardt, B., Lesley, J., Bickel, U., Pardridge, W.M., 2000. Targeting rat anti-mouse transferrin receptor monoclonal antibodies through blood-brain barrier in mouse. J. Pharmacol. Exp. Ther. 292, 1048–1052.
- Lee, H.J., Zhang, Y., Zhu, C., Duff, K., Pardridge, W.M., 2002b. Imaging brain amyloid of Alzheimer disease in vivo in transgenic mice with an Abeta peptide radiopharmaceutical. J. Cereb. Blood Flow Metab. 22, 223–231.
- Litzinger, D.C., Buiting, A.M., van Rooijen, N., Huang, L., 1994. Effect of liposome size on the circulation time and intraorgan distribution of amphipathic poly(ethylene glycol)-containing liposomes. Biochim. Biophys. Acta 1190, 99–107.
- Liu, D., Mori, A., Huang, L., 1992. Role of liposome size and RES blockade in controlling biodistribution and tumor uptake of GM1-containing liposomes. Biochim. Biophys. Acta 1104, 95–101.
- Maruyama, K., Ishida, O., Takizawa, T., Moribe, K., 1999. Possibility of active targeting to tumor tissues with liposomes. Adv. Drug Deliv. Rev. 40, 89–102.
- Matlin, K.S., Reggio, H., Helenius, A., Simons, K., 1982. Pathway of vesicular stomatitis virus entry leading to infection. J. Mol. Biol. 156, 609–631.
- Mori, A., Klibanov, A.L., Torchilin, V.P., Huang, L., 1991. Influence of the steric barrier activity of amphipathic poly(ethyleneglycol) and ganglioside GM1 on the circulation time of liposomes and on the target binding of immunoliposomes in vivo. FEBS Lett. 284, 263–266.
- Omori, N., Maruyama, K., Jin, G., Li, F., Wang, S.J., Hamakawa, Y., Sato, K., Nagano, I., Shoji, M., Abe, K., 2003. Targeting of post-ischemic cerebral endothelium in rat by liposomes bearing polyethylene glycol-coupled transferrin. Neurol. Res. 25, 275–279.
- Pardridge, W.M., 1999. Vector-mediated drug delivery to the brain. Adv. Drug Deliv. Rev. 36, 299–321.
- Ponka, P., Lok, C.N., 1999. The transferrin receptor: role in health and disease. Int. J. Biochem. Cell. Biol. 31, 1111–1137.
- Qian, Z.M., Li, H., Sun, H., Ho, K., 2002. Targeted drug delivery via the transferrin receptor-mediated endocytosis pathway. Pharmacol. Rev. 54, 561–587.
- Rejman, J., Oberle, V., Zuhorn, I.S., Hoekstra, D., 2003. Size-dependent internalization of particles via the pathways of clathrin- and caveolae-mediated endocytosis. Biochem. J.
- Schnyder, A., Krahenbuhl, S., Torok, M., Drewe, J., Huwyler, J., 2003. Targeting of skeletal muscle in vitro using biotinylated immunoliposomes. Biochem. J.
- Shi, N., Boado, R.J., Pardridge, W.M., 2000. Antisense imaging of gene expression in the brain in vivo. Proc. Natl. Acad. Sci. U.S.A. 97, 14709–14714.
- Shi, N., Boado, R.J., Pardridge, W.M., 2001. Receptor-mediated gene targeting to tissues in vivo following intravenous administration of pegylated immunoliposomes. Pharm. Res. 18, 1091–1095.
- Shi, N., Pardridge, W.M., 2000. Noninvasive gene targeting to the brain. Proc. Natl. Acad. Sci. U.S.A. 97, 7567–7572.
- Steven, A.C., Hainfeld, J.F., Wall, J.S., Steer, C.J., 1983. Mass distributions of coated vesicles isolated from liver and brain: analysis by scanning transmission electron microscopy. J. Cell. Biol. 97, 1714–1723.
- Wolburg, H., Lippoldt, A., 2002. Tight junctions of the blood-brain barrier: development, composition and regulation. Vascul. Pharmacol. 38, 323–337.